Infrared Spectroscopic Observation of the Group 13 Metal Hydroxides, $M(OH)_{1,2,3}$ (M = Al, Ga, In, and Tl) and $HAl(OH)_2$

Xuefeng Wang and Lester Andrews*

Chemistry Department, University of Virginia, P.O. Box 400319, Charlottesville, Virginia 22904-4319

Received: September 28, 2006; In Final Form: January 6, 2007

Reactions of laser-ablated Al, Ga, In, and Tl atoms with H_2O_2 and with $H_2 + O_2$ mixtures diluted in argon give new absorptions in the O−H and M−O stretching and O−H bending regions, which are assigned to the metal mono-, di-, and trihydroxide molecules. Isotopic substitutions (D_2O_2, $^{18}O_2$, $^{16,18}O_2$, HD, and D_2) confirm the assignments, and DFT calculations reproduce the experimental results. Infrared spectra for the Al(OH)-(OD) molecule verify the calculated C_{2v} structure. The trihydroxide molecules increase on annealing from the spontaneous reaction with a second H_2O_2 molecule. Aluminum atom reactions with the $H_2 + O_2$ mixtures favor the $HAl(OH)_2$ product, suggesting that AlH_3 generated by UV irradiation combines with O_2 to form $HAl(OH)_2$.

Introduction

The chemistry of aluminum hydroxide is central to geochemistry, environmental science, and medicine.[1−3] In water, tetrahedral $Al(OH)_4^-$ prevails under basic conditions (pH > 7), while in strong acid (pH < 3), the octahedral $Al(H_2O)_6^{3+}$ complex dominates.[2] Pure rotational spectra of the AlOH and AlOD molecules in their ground state and photoionization electronic spectroscopy of AlOH have been reported.[4] The InOH molecule has also been detected through its electronic spectrum in the near-ultraviolet region.[5] Infrared spectra of AlOH, GaOH, and InOH have been observed following the photochemical reaction of metal atoms with H_2O in solid argon.[6,7] In addition, the electronic states of AlOH, GaOH, and InOH have been investigated at high levels of quantum chemical theory, and quasi-linear AlOH and bent GaOH and InOH structures have been found to be the ground states.[8−10] The $Al(OH)_2$ radical has been characterized by ESR in solid neon and by early theoretical calculations,[11,12] but the other molecular $M(OH)_2$ dihydroxides and the $M(OH)_3$ molecules have not been observed experimentally.

In the past three decades, researchers have employed metal atom reactions with H_2O to produce metal hydroxy hydrides and hydroxides. However, the O−H stretching region is often masked by strong H_2O absorptions.[6,7,13] Recently, H_2O_2 has been used in this laboratory as a reagent, and insertion reactions of laser-ablated group 2 and 14 metal (Mg, Ca, Sr, Ba and Sn, Pb) atoms with H_2O_2 have been investigated in solid argon.[14] Numerous metal hydroxides have been identified through M−O and O−H stretching modes without the overlap of strong water absorptions.[15]

In this paper, we report the reactions of laser-ablated group 13 metal atoms with H_2O_2 and identify the products in solid argon. Vibrational frequencies of metal hydroxides, MOH, $M(OH)_2$, and $M(OH)_3$, are identified using isotopic substitution in the infrared spectra and supporting density functional theoretical calculations.

Experimental and Computational Methods

Laser-ablated metal atom reactions with small molecules in excess argon at 10 K have been described in our previous papers.[14−17] The Nd:YAG laser fundamental (1064 nm, 10 Hz repetition rate with 10 ns pulse width) was focused onto a rotating metal target (Johnson Matthey), which gave a bright plume spreading uniformly to the cold CsI window. The solid targets were polished to remove the oxide coating and immediately placed in the vacuum chamber. Gallium was melted into a steel cup for the ablation target. The laser energy was varied to about 10−20 mJ/pulse. FTIR spectra were recorded at 0.5 cm^{-1} resolution on Nicolet 750 with a 0.1 cm^{-1} frequency accuracy using an MCTB detector. Matrix samples were annealed at different temperatures, and selected samples were subjected to photolysis by a medium-pressure mercury arc lamp (Philips, 175W) with the globe removed.

Urea hydrogen peroxide (UHP) (Aldrich, 98%) was used to provide pure H_2O_2 vapor. This solid material was placed in a glass tube at room temperature and pumped for about 1 h to remove H_2O. Argon gas was passed over the UHP, which released H_2O_2 to mix with excess argon on deposition. Deuteriated urea-D_2O_2 was prepared following the method of Pettersson et al.[18,19] Additional experiments were done with samples of H_2, D_2, or HD and O_2, $^{18}O_2$, or $^{16,18}O_2$ mixtures.

Complementary DFT calculations were performed using the Gaussian 03 program system,[20] the B3LYP density functional, the 6-311+G(3df,3pd) basis set for hydrogen, oxygen, aluminum, and gallium atoms, and SDD pseudopotential and basis for indium and thallium atoms.[21−23] All of the geometrical parameters were fully optimized, and the harmonic vibrational frequencies were obtained analytically at the optimized structures. Anharmonic frequencies were also calculated for comparison.[24]

Results

Infrared spectra of products formed in the reactions of laser-ablated group 13 atoms with H_2O_2 or H_2 and O_2 mixtures in excess argon during condensation at 10 K will be presented in turn. Density functional calculations were performed to support the identifications of new reaction products. Common species, such as water, O_3, O_4^-, HO_2, Ar_nH^+, and the HOH−O complex have been identified in previous papers.[19,25−30]

Al + H_2O_2 and Al + H_2 + O_2. Infrared spectra of laser-ablated aluminum atoms co-deposited with H_2O_2 in excess argon

* Corresponding author. Email: lsa@virginia.edu.

10.1021/jp066390e CCC: $37.00
Published on Web 02/22/2007

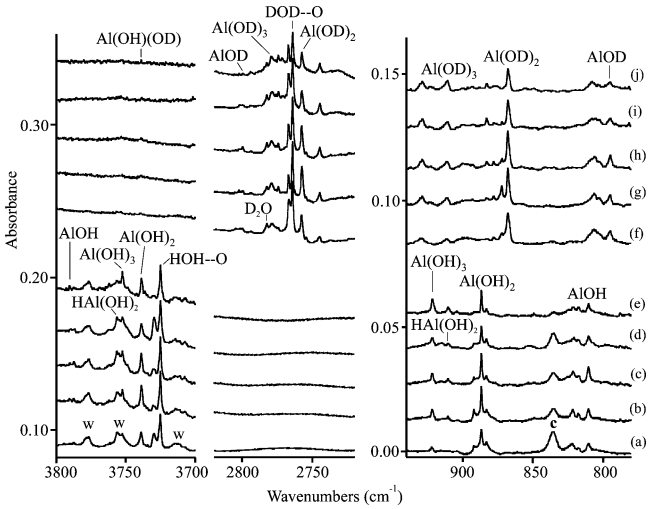

Figure 1. Infrared spectra for laser-ablated aluminum atom and H_2O_2 reaction products in solid argon at 10 K. (a) Al + H_2O_2 deposition for 60 min, (b) after annealing to 20 K, (c) after 240−380 nm irradiation, (d) after >220 nm irradiation, (e) after annealing to 30 K, (f) Al + D_2O_2 deposition for 60 min, (g) after annealing to 20 K, (h) after 240−380 nm irradiation, (i) after >220 nm irradiation, and (j) after annealing to 30 K. The sharp, weak 2744.6 cm^{-1} band is common to laser-ablation experiments with D_2O_2. The label w denotes water absorptions.

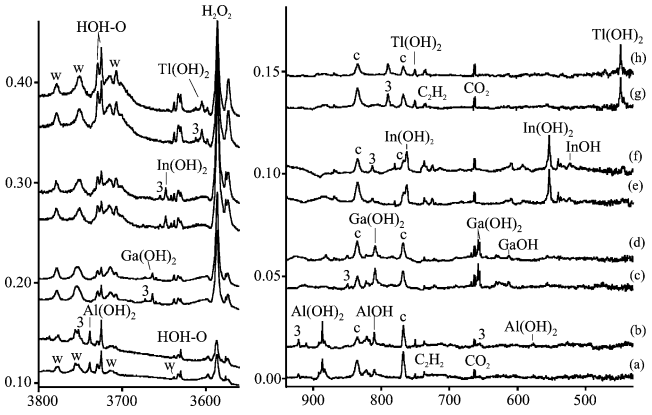

Figure 2. Infrared spectra for laser-ablated Al, Ga, In, and Tl atoms and H_2O_2 reaction products in solid argon at 10 K. (a) Al + H_2O_2 deposition for 60 min, (b) after 240−380 nm irradiation, (c) Ga + H_2O_2 deposition for 60 min, (d) after 240−380 nm irradiation, (e) In + H_2O_2 deposition for 60 min, (f) after 240−380 nm irradiation, (g) Tl + H_2O_2 deposition for 60 min, and (h) after 240−380 nm irradiation. The spectra after irradiation were selected to optimize the $M(OH)_2$ products: the weak bands labeled 3 are due to the $M(OH)_3$ products, which increase on annealing.

at 10 K, with annealing and photolysis afterward, gave three new O−H stretching frequencies at 3787.0, 3752.4, and 3738.7 cm^{-1}, three new Al−O stretching frequencies at 921.5, 886.7, and 810.4 cm^{-1}, and weak O−H bending absorptions at 655.0 and 576.7 cm^{-1} (Figures 1 and 2). The bands labeled c at 835.4 cm^{-1} (and at 767.7 cm^{-1} in later figures) are common to these hydrogen peroxide experiments and are likely due to a precursor complex. With D_2O_2, the counterpart O−D stretching bands were found at 2799.8, 2767.1, and 2757.6 cm^{-1} with a sharp 2782.4 cm^{-1} band for D_2O, Al−O stretching absorptions at 910.9, 867.8, and 794.7 cm^{-1} (Figure 1), and an O−D bending band at 469.1 cm^{-1}. The sharp, weak 2744.6 cm^{-1} band is common to laser-ablation experiments with D_2O_2, and since it is in the region for D_2O absorption, it is likely due to a D_2O complex formed in these experiments. A group of weak bands at 3755.0, 1935.1, 910.4, and 511.7 cm^{-1} was also observed in Al + H_2O_2 experiments, which are the major product bands in

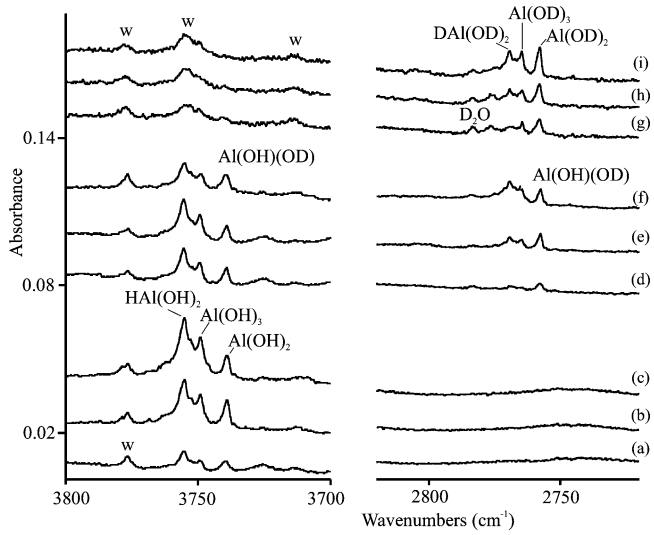

Figure 3. Infrared spectra for the aluminum atom reaction products with oxygen and hydrogen isotopic mixtures in solid argon at 10 K. (a) Al + 0.5% O_2 + 5% H_2 deposition for 60 min, (b) after 240−380 nm irradiation, (c) after >220 nm irradiation, (d) Al + 0.5% O_2 + 5% HD deposition for 60 min, (e) after 240−380 nm irradiation, (f) after >220 nm irradiation, (g) Al + 0.5% O_2 + 5% D_2 deposition for 60 min, (h) after 240−380 nm irradiation, and (i) after >220 nm irradiation.

TABLE 1: Infrared Absorptions (cm^{-1}) Observed in Solid Argon for Products of the Reactions of Al Atoms with H_2O_2 or H_2 + O_2 Molecules

$H_2O_2/H_2 + O_2$	$D_2O_2/D_2 + O_2$	$H_2 + {}^{18}O_2$	$D_2 + {}^{18}O_2$	identification
3787.0	2799.8			AlOH
3755.0/3755.0	2769.4/2769.4	3743.2	2752.1	$HAl(OH)_2$
3752.4/3749.2	2767.1/2764.6		2747.9	$Al(OH)_3$
3738.7/3739.1	2757.6/2757.9		2740.8	$Al(OH)_2$
1935.1/1935.7	−/1411.5	1935.7	1411.5	$HAl(OH)_2$
921.5	910.9			$Al(OH)_3$
910.4/911.4	−/893.5	889.9	870.2	$HAl(OH)_2$
886.7/886.9	867.8/868.0	865.5	846.4	$Al(OH)_2$
810.4	794.7			AlOH
655.0				$Al(OH)_3$
576.7	468.3			$Al(OH)_2$
511.7	465.3	510.7		$HAl(OH)_2$

the Al + H_2 + O_2 investigations. Weak oxide absorptions of cyc-AlO_2 at 496.3 cm^{-1}, Al−O−Al at 992.8 cm^{-1}, and $(AlO)_x$ at 1145.1 and 1129.5 cm^{-1} were observed that are partly from metal oxide on the target surface and partly from decomposition of aluminum hydroxides.[31] Table 1 shows the aluminum reaction product absorptions.

Reactions of laser-ablated Al with the H_2 + O_2 mixture gave a group of new product bands at 3755.0, 1935.7, 911.4, and 511.7 cm^{-1}, in addition to analogous bands from Al + H_2O_2 experiments but now with very low intensities. The upper region is compared in Figure 3 for Al and H_2, HD or D_2 and O_2 reaction products. The weak 3752.4 cm^{-1} band (with H_2) now has a stronger 3749.2 cm^{-1} counterpart, and the weak 2767.7 cm^{-1} band (with D_2) now has stronger 2764.6 cm^{-1} counterpart. Both of these regions reveal the same bands with HD, except that the lower bands shift slightly to 3739.5 and to 2757.5 cm^{-1}. The lower region is compared in Figure 4 for Al and H_2 reactions with oxygen isotopes. It is no surprise that strong aluminum hydride bands were observed at 1882.6, 783.5, and 697.8 cm^{-1} (AlH_3), at 1806.0 and 1769.4 cm^{-1} (AlH_2), and at 1590.7 cm^{-1} (AlH).[32] The deuterium counterpart of the 1935.7 cm^{-1} band is observed at 1411.5 cm^{-1} (Table 1).

Ga + H_2O_2 and Ga + H_2 + O_2. The Ga + H_2O_2 experiments produced gallium hydroxide absorptions at 3689.5,

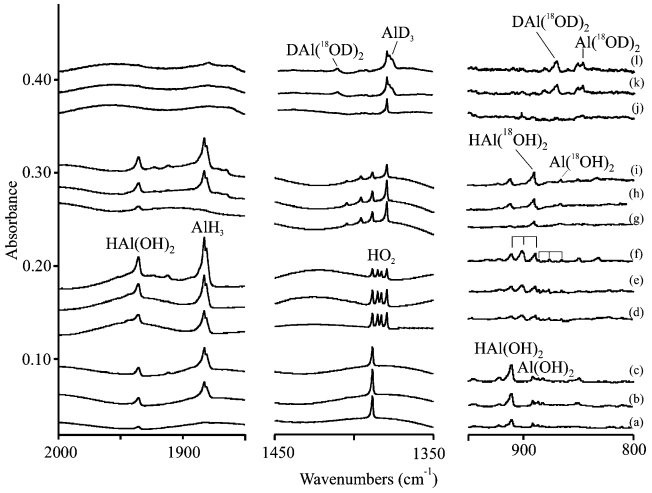

Figure 4. Infrared spectra for the aluminum atom reaction products with oxygen and hydrogen mixtures in solid argon at 10 K. (a) Al + 0.5% O_2 + 5% H_2 deposition for 60 min, (b) after 240−380 nm irradiation, (c) after >220 nm irradiation, (d) Al + 0.15% $^{16}O_2$ + 0.3%^{16,18} O_2 + 0.15% $^{18}O_2$ + 5% H_2 deposition for 60 min, (e) after 240−380 nm irradiation, (f) after >220 nm irradiation, (g) Al + 0.5% $^{18}O_2$ + 5% H_2 deposition for 60 min, (h) after 240−380 nm irradiation, (i) after >220 nm irradiation, (j) Al + 0.5% $^{18}O_2$ + 5% D_2 deposition for 60 min, (k) after 240−380 nm irradiation, and (l) after >220 nm irradiation.

3672.4, and 3663.8 cm^{-1} (O−H stretching region), gallium isotopic doublets at 721.4 and 719.1, 657.2 and 655.2, and 612.9 and 611.3 cm^{-1} (Ga−O stretching region), and bands at 850.1 and 809.2 cm^{-1} (O−H bending region). With Ga + D_2O_2, these bands shift to 2720.1, 2708.3, and 2702.6 cm^{-1} (O−D stretching), gallium isotopic doublets at 720.7 and 718.3, 647.5 and 646.5, and 595.9 and 594.2 cm^{-1} (Ga−O stretching), and bands at 658.6 and 656.1 cm^{-1} (O−D bending). These absorptions are illustrated in Figures 2 and 5. Weak metal oxide appeared at 822.8 cm^{-1} in both H_2O_2 and D_2O_2 experiments.[33] Investigations with H_2 + O_2 and D_2 + O_2 gave weak absorptions for GaH at 1513.9 cm^{-1} and GaD at 1090.5 cm^{-1}, respectively,[34,35] and gallium oxide absorptions.[33] However, no gallium hydroxide product bands were observed.

In + H_2O_2 and In + H_2 + O_2. Laser-ablated In atom reactions with H_2O_2 in excess argon gave new absorptions in the O−H stretching region at 3675.5, 3654.7, and 3647.8 cm^{-1}, in the O−H bending region at 812.9 and 762.3 cm^{-1}, and in the In−O stretching region at 608.2, 552.7, and 522.7 cm^{-1}. Experiments with D_2O_2 produced new bands in the O−D stretching region at 2708.3, 2695.3, and 2690.8 cm^{-1}, in the O−D bending region at 620.3 and 579.0 cm^{-1}, and in the In−O stretching region at 551.9, 531.4, and 505.8 cm^{-1}. Figures 2 and 6 illustrate these absorptions. No indium hydroxide absorptions were observed in the H_2 + O_2 and D_2 + O_2 experiments, but weak indium dioxide (OInO) at 755.5 cm^{-1} and indium monohydride InH at 1387.4 cm^{-1} and InD at 995.9 cm^{-1} absorptions were detected.[33,35]

Tl + H_2O_2. New absorptions from Tl atom reactions with H_2O_2 were observed at 3612.1, 3604.6, 790.3, 750.6, and 447.9 cm^{-1}. With D_2O_2, these bands shifted to 2664.6, 2659.4, 590.4, 551.1, and 444.9 cm^{-1}. No thallium oxide absorptions were observed.[36] Figure 2 compares hydrogen peroxide reaction products for the four group 13 metal atoms and shows the metal dependence on the product absorptions.

B + H_2O_2. To complete group 13, boron atom reactions with H_2O_2 were also investigated using natural boron and targets enriched in both boron-10 and boron-11. We observed only

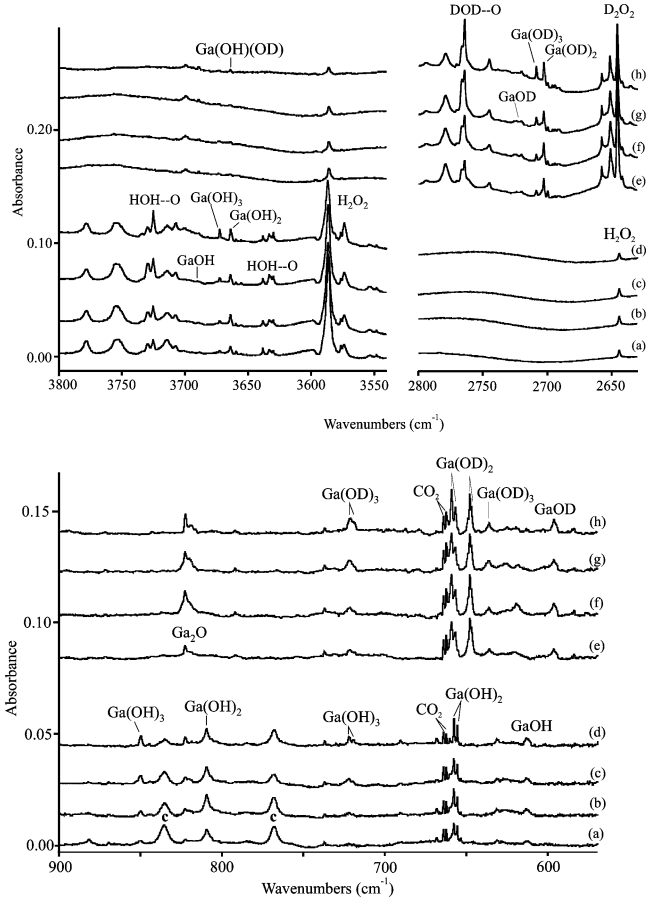

Figure 5. Infrared spectra for laser-ablated gallium atom and H_2O_2 reaction products in solid argon at 10 K. (a) Ga + H_2O_2 deposition for 60 min, (b) after 240−380 nm irradiation, (c) after >220 nm irradiation, (d) after annealing to 20 K, (e) Ga + D_2O_2 deposition for 60 min, (f) after 240−380 nm irradiation, (g) after >220 nm irradiation, and (h) after annealing to 20 K.

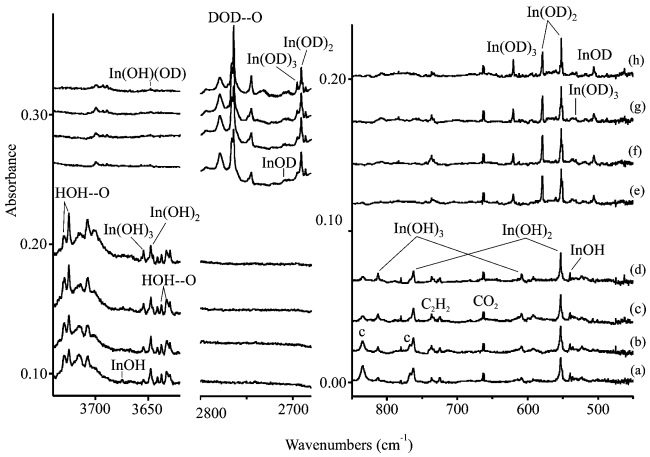

Figure 6. Infrared spectra for laser-ablated indium atom and H_2O_2 reaction products in solid argon at 10 K. (a) In + H_2O_2 deposition for 60 min, (b) after 240−380 nm irradiation, (c) after >220 nm irradiation, (d) after annealing to 20 K, (e) In + D_2O_2 deposition for 60 min, (f) after 240−380 nm irradiation, (g) after >220 nm irradiation, and (h) after annealing to 20 K.

weak absorptions for BO, HBO, and BH, which have been identified in previous experiments.[37] In particular, no evidence was found for $B(OH)_3$ nor HOBO.[38]

Calculations. Calculations were done for the MOH, $M(OH)_2$, and $M(OH)_3$ hydroxide molecules at the B3LYP level of theory to support the identification of the new IR product absorptions,

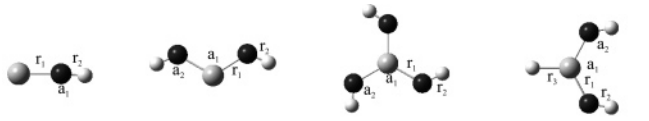

Al: r_1=1.686 r_2=0.952 a_1=175	r_1=1.707; r_2=0.957 a_1=116; a_2=124	r_1=1.694; r_2=0.956 a_1=120; a_2=124	r_1=1.698; r_2=0.955 r_3=1.557 a_1=124; a_2=128
Ga: r_1=1.783 r_2=0.965 a_1=155	r_1=1.813; r_2=0.961 a_1=113; a_2=114	r_1=1.786; r_2=0.961 a_1=120; a_2=114	r_1=1.797; r_2=0.960 r_3=1.537 a_1=120; a_2=117
In: r_1=1.986 r_2=0.957 a_1=142	r_1=1.975; r_2=0.960 a_1=113; a_2=117	r_1=1.940; r_2=0.959 a_1=120; a_2=117	
Tl: r_1=2.110 r_2=0.960 a_1=126	r_1=2.102; r_2=0.963 a_1=116; a_2=112	r_1=2.022; r_2=0.962 a_1=120; a_2=112	

Figure 7. Structures calculated for group 13 metal hydroxide molecules using B3LYP/6-311++G(3df,3pd) for Al and Ga with SDD for In and Tl. Bond lengths in angstroms and angles in degrees.

and the metal hydroxide structures are illustrated in Figure 7. Two stable conformers for $M(OH)_2$, namely, C_s, *cis*−*trans* $M(OH)_2$, and C_{2v}, *trans*−*trans*-$M(OH)_2$, were found with very close energies, while all $M(OH)_3$ molecules converged to C_{3h} symmetry structures. Calculated frequencies are listed in Tables 2−4 for comparison with observed values. In addition, the $HAl(OH)_2$ molecule was also computed and found to have a C_{2v} symmetry structure, and the calculated frequencies are listed in Table 5.

Discussion

The new group 13 metal hydroxide molecules will be identified through different reaction mixtures, photochemical properties, isotopic substitution, and comparison with theoretical frequency calculations for the anticipated product molecules.

MOH. A weak band at 810.7 cm^{-1} in the Al−O stretching region appeared on deposition of laser-ablated Al atoms with H_2O_2 in excess argon, increased by 100% on 240−380 nm irradiation, and decreased by 50% on >220 nm irradiation, which tracked a weak O−H stretching mode at 3787.0 cm^{-1}. With D_2O_2, the Al−O and O−H stretching modes shifted to 794.7 and 2799.8 cm^{-1}, respectively, defining 1.0201 and 1.3526 H/D isotopic frequency ratios. The O−H stretching mode was typical of that found in many metal hydroxide molecules,[14,15] and the Al−O stretching mode may be coupled with the lower frequency Al−O−H bending mode. The observed AlOH absorptions are in agreement with early assignments of Hauge et al.,[6] and our work supports their identification of AlOH. In addition, the previous AlOH absorptions are compatible with the B3LYP frequencies reported in Table 5, which were calculated to correlate with the $Al(OH)_{1,2,3}$ product frequencies. The anharmonic calculation brings the harmonic O−H stretching frequency down to near the observed value, and the calculated harmonic and anharmonic Al−O stretching values bracket the observed frequency. Finally, the highest level calculation[8] for AlOH predicts 831 cm^{-1}, which is in good agreement with the argon matrix 810.7 cm^{-1} value for the Al−O stretching mode.

A weak 895 cm^{-1} hot band in the photoionization electronic spectrum of AlOH has been assigned to the Al−O stretching fundamental.[4b] This assignment represents an extraordinarily large 9.4% matrix shift for the 810.7 cm^{-1} absorption, which casts doubt on the gas-phase hot band assignment. Furthermore, the recent highest level calculation predicts this mode at 831 cm^{-1}, in excellent agreement with the argon matrix assignment. The original Rice work is supported by oxygen-18 isotopic shifts for this Al−O stretching mode, and the matrix identifications of AlOH appear to be substantiated.

In the Ga + H_2O_2 experiments, absorptions due to GaOH were found at 3689.5 cm^{-1} (O−H stretching) and 612.9 cm^{-1} (^{69}Ga−O stretching) and 611.3 cm^{-1} (^{71}Ga−O stretching), which appeared on deposition, increased slightly on irradiation, and disappeared on further annealing. The deuterium counterparts were found at 2720.1 and 595.9 cm^{-1}, giving 1.3558 and 1.0591 H/D ratios. These absorptions are essentially the same as earlier argon matrix observations,[6,7] which supports their assignment to GaOH as do the present and recent frequency calculations.[7,9]

The laser-ablated In atom reaction with H_2O_2 gave two weak bands at 3675.5 and 522.7 cm^{-1}, respectively, which appeared on deposition and decreased on irradiation and annealing. With D_2O_2, the counterparts were found at 2708.3 and 505.8 cm^{-1}, giving 1.3571 and 1.0670 H/D ratios. These bands are appropriate for InOH based on previous work.[6] The InOH is identified in the gas phase from its electronic spectrum in the near-UV region, and In−O stretching modes for InOH and InOD were determined as 542 and 525 cm^{-1}, respectively,[5] which are in very good agreement with our argon matrix values and those from the Rice group.[6]

No band was observed for TlOH in laser-ablated Tl reactions with H_2O_2. However, the 447.9 cm^{-1} absorption tentatively assigned to TlOH from the Tl/water photochemical reaction by Hauge et al.[6] is in fact the major absorption observed here from the H_2O_2 reaction, and this band will be assigned to $Tl(OH)_2$.

DFT calculations support these assignments and provide an important correlation with the higher hydroxides. The results of our DFT calculations are in accord with recent computations using higher levels of theory.[8−10] At the B3LYP level of theory, the harmonic O−H stretching modes of MOH are predicted at 3984.2 cm^{-1} (AlOH), 3890.7 cm^{-1} (GaOH), and 3916.2 cm^{-1} (InOH), which are overestimated by 5.2, 5.5, and 6.5%, respectively. However, with anharmonic frequency calculations, the percent deviations are reduced to 1.3, 0.0, and −0.3%, respectively, for this simple O−H stretching mode. The M−O stretching modes are calculated at 821.7 cm^{-1} (AlOH), 615.1 cm^{-1} (GaOH), and 554.8 cm^{-1} (InOH), which are overestimated by 1.4, 0.5, and 6.1%, respectively.

The MOH molecules are generated from decomposition of the energized $[M(OH)_2]^*$ intermediate before it was relaxed by the cold matrix, reaction 1. Overall, reaction 1 is exothermic by 81, 62, 56, and 42 kcal/mol for Al, Ga, In, and Tl, respectively, calculated at the B3LYP level of theory.

$$M + H_2O_2 \rightarrow [M(OH)_2]^* \rightarrow MOH + OH \qquad (1)$$

Another equilibrium structure, HMO, has been studied theoretically, and this is located at substantially higher energies.[8−10] There is no evidence for these higher energy metal species in our experiments. However, HBO is calculated to be 62 kcal/mol lower in energy than BOH, and weak HBO bands are observed in experiments with boron atoms and hydrogen peroxide.

$M(OH)_2$. The new bands at 3738.7, 886.7, and 576.7 cm^{-1} track together in Al + H_2O_2 experiments. With D_2O_2, these bands appeared at 2774.3, 867.8, and 469.1 cm^{-1}, respectively. The H/D frequency ratios show that the 3738.7 cm^{-1} band is appropriate for the O−H stretching mode (H/D = 3738.7:2757.6 = 1.3558),[14,15] the 886.7 cm^{-1} band is due to the Al−O stretching mode coupled slightly with hydrogen/deuterium (886.7:867.8 = 1.0218), and the 576.7 cm^{-1} band is due to the Al−O−H bending mode, which exhibits an intermediate H/D ratio (576.7:469.1 = 1.2294). Experiments with H_2 + O_2 gave very weak bands at 3739.1 and 886.9 cm^{-1}, which were

TABLE 2: Observed and Calculated Frequencies (cm^{-1}) for MOH (M = Al, Ga, In, and Tl) Molecules ($^1A'$ State)

	calcd[a]		obsd	calcd	obsd	calcd		obsd	calcd	obsd
	harm	anharm				harm	anharm			
	AlOH			AlOD		GaOH			GaOD	
OH stretch	3984.2 (55)[b]	3837.1	3787.0	2908.2 (52)	2799.8	3890.7 (48)	3695.3	3689.5	2836.7 (46)	2720.1
MO stretch	821.7 (153)	807.3	810.7	805.3 (146)	794.7	615.1 (152)	606.1	612.9	599.4 (150)	595.9
MOH bend	34.2 (179)[c]	437.1i		27.3 (98)		63.9 (146)	428.8		25.8 (83)	
	InOH			InOD		TlOH			TlOD	
OH stretch	3916.2 (27)	3764.5	3675.5	2853.7 (27)	2708.3	3867.8 (18)	3709.7		2816.5 (18)	
MO stretch	554.8 (113)	562.6	522.7	537.6 (121)	505.8	391.5 (154)	377.4		330.6 (45)	
MOH bend	260.4 (93)	88.2		195.2 (51)		477.7 (11)	445.0		408.5 (108)	

[a] B3LYP/6-311++G(3df,3pd) for Al and Ga with SDD for In and Tl. [b] Intensities, km/mol. [c] The M−O−H bending mode is more difficult to model, and as a result, the anharmonic frequency does not follow the expected relationship with the harmonic result.

TABLE 3: Observed and Calculated Frequencies (cm^{-1}) for $M(OH)_2$ (C_{2v}) (M = Al, Ga, In, and Tl) Molecules ($^2A_1$ State)

calcd[a]		obsd	calcd	obsd	calcd		obsd	calcd	obsd
harm	anharm				harm	anharm		harm	
$Al(OH)_2$			$Al(OD)_2$			$Ga(OH)_2$		$Ga(OD)_2$	
3924.6 (b_2, 175)[b]	3725.8	3738.7	2857.2 (112)	2757.6	3860.4 (a_1, 1)	3690.9		2811.4 (0)	
3924.2 (a_1, 1)	3725.2		2857.8 (1)		3860.0 (b_2, 147)	3690.7	3663.8	2810.2 (118)	2702.6
886.9 (b_2, 95)	873.1	886.7	866.4 (139)	867.9	820.1 (a_1, 124)	811.7	809.2	640.9 (118)	658.6, 656.1
737.6 (a_1, 28)	726.5		725.7 (69)		768.4 (b_2, 49)	770.0		569.7 (2)	
634.4 (a_1, 201)	528.3	576.7	478.8 (101)	469.1	641.4 (b_2, 154)	628.5	657.2, 655.2	638.7 (109)	647.5, 646.5
574.5 (b_2, 172)	421.4		436.0 (80)		607.7 (a_1, 30)	591.4		560.6 (48)	
331.7 (b_1, 153)	150.2		240.4 (80)		316.8 (b_1, 155)	397.0		226.6 (82)	
277.5 (a_2, 0)	81.0		218.9 (1)		265.0 (a_2, 0)	382.0		199.7 (0)	
231.8 (a_1, 3)	222.8		211.6 (0)		180.0 (a_1, 2)	184.6		171.1 (1)	
$In(OH)_2$			$In(OD)_2$			$Tl(OH)_2$		$Tl(OD)_2$	
3873.6 (a_1, 0)	3686.0		2821.1 (0)		3831.6 (a_1, 0)	3683.4		2790.1 (0)	
3873.1 (b_2, 119)	3685.7	3647.8	2820.1 (78)	2690.8	3829.8 (b_2, 133)	3681.7	3604.6	2788.3 (81)	2659.4
721.5 (a_1, 122)	676.1	762.3	565.6 (98)	579.0	786.7 (a_1, 110)	812.0	750.6	582.0 (76)	551.1
671.5 (b_2, 22)	639.8		512.4 (7)		732.4 (b_2, 43)	767.6		532.7 (29)	
564.7 (b_2, 134)	552.0	552.7	556.9 (104)	551.9	397.1 (b_2, 61)	387.3	447.9	393.8 (55)	444.9
543.6 (a_1, 33)	532.7		486.0 (35)		374.0 (a_1, 17)	363.2		365.6 (12)	
285.6 (b_1, 148)	267.3		204.3 (81)		231.6 (b_2, 152)	460.9		165.1 (82)	
250.7 (a_2, 0)	240.6		188.2 (0)		201.2 (a_2, 0)	475.4		150.7 (0)	
146.1 (a_1, 4)	143.9		138.9 (4)		114.0 (a_1, 2)	132.8		108.8 (2)	

[a] B3LYP/6-311++G(3df,3pd) for Al and Ga with SDD for In and Tl. [b] Mode symmetries C_{2v}; intensities, km/mol.

TABLE 4: Observed and Calculated Frequencies (cm^{-1}) for $M(OH)_3$ (C_{3h}) (M = Al, Ga, In, and Tl) ($^1A'$ State)

calcd[a]	obsd	calcd	obsd	calcd	obsd	calcd	obsd
$Al(OH)_3$		$Al(OD)_3$		$Ga(OH)_3$		$Ga(OD)_3$	
3936.1 (a, 0)[b]		2867.4 (0)		3863.3 (a, 0)		2813.2 (0)	
3934.6 (e, 1182)	3752.4	2865.4 (822)	2767.0	3861.7 (e, 952)	3672.4	2811.2 (652)	2708.3
930.6 (e, 1762)	921.5	910.1 (2142)	910.9	861.2 (e, 1212)	850.1	638.2 (302)	635.6
705.1 (a, 0)		674.1 (0)		831.9 (a, 0)		647.9 (0)	
639.6 (e, 2192)	655.0	503.5 (1032)		713.7 (e, 1262)	721.4, 719.1	714.2 (1682)	720.7, 718.3
627.4 (a, 0)		474.6 (0)		644.8 (a, 0)		596.2 (0)	
361.0 (e, 02)		269.1 (02)		342.1 (e, 02)		253.9 (02)	
329.3 (a, 388)		301.9 (180)		304.9 (a, 290)		230.6 (199)	
290.7 (a, 7)		229.0 (88)		202.8 (a, 26)		192.0 (0)	
225.6 (e, 292)		205.4 (272)		169.0 (e, 222)		158.6 (202)	
$In(OH)_3$		$In(OD)_3$		$Tl(OH)_3$		$Tl(OD)_3$	
3881.9 (a, 0)		2827.2 (0)		3850.6 (a, 0)		2803.9 (0)	
3881.3 (e, 802)	3654.7	2826.0 (572)	2695.3	3849.4 (e, 752)	3612.1	2802.4 (522)	2664.6
748.5 (e, 992)	812.9	632.6 (1202)	620.3	877.2 (e, 862)	790.3	646.7 (632)	590.4
727.6 (a, 0)		590.8 (0)		860.9 (a, 0)		625.3 (0)	
635.7 (e, 1132)	608.2	554.5 (502)	531.4	488.4 (e, 832)		482.1 (752)	
594.7 (a, 0)		526.8 (0)		479.4 (a, 0)		473.9 (0)	
302.6 (e, 02)		224.3 (02)		295.0 (e, 02)		218.0 (02)	
278.0 (a, 256)		207.0 (188)		279.9 (a, 246)		204.9 (161)	
163.6 (a, 34)		156.8 (8)		143.7 (a, 30)		139.7 (15)	
143.2 (e, 242)		134.7 (212)		114.0 (e, 242)		108.3 (211)	

[a] B3LYP/6-311++G(3df,3pd) for Al and Ga with SDD for In and Tl. [b] Mode symmetries C_{3h}; intensities, km/mol.

observed on deposition, increased slightly on >290 nm irradiation, and decreased on further annealing. With $H_2 + {}^{18}O_2$, these two bands shifted to 3727.8 and 865.5 cm^{-1}, respectively, which clearly supports the O−H and Al−O stretching mode assignments. With $D_2 + {}^{18}O_2$, additional isotopic data were observed at 2740.9 and 846.4 cm^{-1}. The oxygen 16:18 isotopic ratios for the two hydrogen isotopic molecules were 1.0247 and 1.0255, which are just below the 1.0261 value for OAlO.[31] Experiments with $H_2 + {}^{16}O_2/{}^{16,18}O_2/{}^{18}O_2$ gave a doublet at 3739 and 3728 cm^{-1} for the O−H stretching mode and a triplet at

TABLE 5: Observed and Calculated Frequencies (cm^{-1}) for $HAl(OH)_2$ in C_{2v} Symmetry $^1A_1$ Ground State

$HAl(OH)_2$		$DAl(OD)_2$		$HAl(^{18}OH)_2$	
calcd[a]	obsd	calcd	obsd	calcd	obsd
3944.6 (a_1, 104)[b]	3755.0	2873.7 (75)	2769.4	3931.5 (99)	3743.2
3942.1 (b_2, 34)		2872.0 (25)		3928.9 (32)	
2030.4 (a_1, 106)	1935.7	1463.2 (74)	1411.5	2030.4 (106)	1935.7
901.1 (b_2, 177)	911.4	887.9 (217)	893.5	878.1 (162)	889.9
799.3 (a_1, 76)		754.9 (69)		778.1 (71)	
675.4 (b_2, 186)		493.7 (109)		673.2 (179)	
608.5 (a_1, 1)		497.5 (6)		592.6 (2)	
547.1 (b_2, 222)	511.7	402.9 (98)	465.3	543.7 (225)	510.5
513.9 (b_1, 47)		394.8 (77)		513.6 (44)	
357.8 (b_1, 321)		286.8 (154)		353.2 (318)	
309.1 (a_2, 0)		226.3 (0)		307.8 (0)	
251.3 (a_1, 30)		224.7 (23)		243.9 (29)	

[a] B3LYP/6-311++G(3df,3pd) level of theory. [b] Mode symmetries C_{2v}; intensities, km/mol.

886.9, 877.1, and 865.5 cm^{-1} for the Al−O stretching mode (Figure 4). Accordingly, these bands are assigned to the Al(OH)$_2$ molecule where the Al−O stretching modes couple to reveal two equivalent oxygen atoms, but the O−H stretching modes do not couple owing to motion in the latter being predominantly hydrogen and the former oxygen.

Infrared absorptions of Ga(OH)$_2$ were observed at 3663.8 cm^{-1} (O−H stretching), 809.2 cm^{-1} (O−H bending), and a gallium isotopic doublet at 657.2 and 655.2 cm^{-1} (Ga−O stretching) in laser-ablated Ga atom reactions with H_2O_2 in solid argon. The 657.2 and 655.2 cm^{-1} doublet pattern is appropriate for ^{69}Ga and ^{71}Ga in natural abundance as this splitting is calculated to be 2.1 cm^{-1}. With D_2O_2, these bands shift to 2702.6 cm^{-1} (O−D stretching, H/D = 1.3557), and two doublets now appeared at 658.6 and 656.1 cm^{-1} and at 647.5 and 646.5 cm^{-1} (Ga−O−D bending mixed with Ga−O stretching with ^{69}Ga and ^{71}Ga splittings). The mixed H_2O_2 and D_2O_2 reactions produced the same product bands as the pure isotopic precursors, which shows that a single hydrogen peroxide molecule reacts to give this new product.

Experiments with In + H_2O_2 gave a group of bands at 3647.8, 762.3, and 552.7 cm^{-1}, which are appropriate for the In(OH)$_2$ molecule. With D_2O_2, these bands shifted to 2690.8, 579.0, and 551.9 cm^{-1}, respectively. The H/D frequency ratios were 1.3557, 1.3166, and 1.0014, respectively.

The absorptions due to the Tl(OH)$_2$ molecule are identified as an O−H stretching mode at 3604.6 cm^{-1}, an O−H bending mode at 750.6 cm^{-1}, and a Tl−O stretching mode at 447.9 cm^{-1} upon deposition of laser-ablated Tl atoms with H_2O_2 in solid argon. With D_2O_2, the O−D stretching mode appears at 2659.4 cm^{-1}, giving the 1.3554 H/D ratio, which is very close to the analogous mode ratios for Al(OH)$_2$, Ga(OH)$_2$, and In(OH)$_2$. The Tl−O stretching mode red-shifts 3.0 to 444.9 cm^{-1}, indicating very little coupling of the O−D bending vibration with the Tl−O stretching mode. In addition, the O−D bending mode is observed at 551.1 cm^{-1} and defines a H/D frequency ratio of 1.3620, which is higher than this mode ratio for the lighter group 13 dihydroxide bending modes and indicates decreasing bending mode anharmonicity going down the family. With H_2O_2 + D_2O_2, the bands due to both Tl(OH)$_2$ and Tl(OD)$_2$ were found to be exactly the same as the bands discussed previously, which shows that the reaction proceeds with a single H_2O_2 molecule.

Two structures for the M(OH)$_2$ molecules, namely, the C_s cis−trans and the C_{2v} trans−trans, have virtually the same energy at the B3LYP level of theory, but the frequencies are clearly different, particularly for the two O−H stretching modes. Calculated frequencies in Table 2 for the C_{2v} structures show that the strong b_2 mode is predicted to be 0.4 cm^{-1} higher than the very weak a_1 mode for Al(OH)$_2$, but this relationship is reversed for the Ga and In dihydroxides, and the deuteriated counterparts all have slightly lower strong b_2 modes. Within the accuracy of the calculations, the two stretching modes of these equivalent O−H subunits are very close, within 1 cm^{-1}. However, the C_s structure has two different uncoupled O−H stretching modes, which are calculated at 3920.5 cm^{-1} (81 km/mol intensity) and 3886.5 cm^{-1} (45 km/mol) for the Al species, and the other metals follow suit. Our spectra clearly show that the region 34 cm^{-1} below the strong Al(OH)$_2$ band is free of significant absorption. Furthermore, the HD experiment finds two strong modes for Al(OH)(OD) at 3739.5 and 2757.5 cm^{-1}, which are 0.4 cm^{-1} higher and lower, respectively, than the corresponding strong bands for the pure isotopic species listed in Table 1. This clearly shows that the two O−H (or O−D) bonds are equivalent as there is only a very small shift when these modes uncouple as they must in Al(OH)(OD). In the C_1 case, the two O−H bonds are essentially uncoupled, and the mixed isotopic molecules have one each of the same modes as the pure isotopic molecules, which is not in agreement with our experimental observations. Hence, our IR spectra clearly show that the Al(OH)$_2$ molecule has the equivalent O−H ligands required for C_{2v} symmetry. On the basis of the observation of Ga(OH)(OD) at 3664.1 cm^{-1}, slightly above Ga(OH)$_2$ at 3663.8 cm^{-1}, and In(OH)(OD) at 3648.2 cm^{-1}, just 0.4 cm^{-1} above In(OH)$_2$, such C_{2v} structures are substantiated here for these heavier group 13 dihydroxide molecules. Figure 7 illustrates the structures for these dihydroxide molecules and lists the structural parameters.

Earlier electronic structure calculations on the Al(OH)$_2$ radical found the cis−trans structure to be the lowest in energy by about 1 kcal/mol, but this is surely within the energy uncertainty of these calculations.[12] In addition, the nuclear hyperfine constants calculated for these two possible structures bracket the experimental ESR values in solid neon but are closer to the cis−trans data.[11] These authors appear to favor the cis−trans structure, but they appreciate that such a choice is not definitive.

The DFT frequency calculations predict strong OH antisymmetric stretching modes at 3924.6 cm^{-1} for Al(OH)$_2$, 3860.0 cm^{-1} for Ga(OH)$_2$, 3873.1 cm^{-1} for In(OH)$_2$, and 3829.8 cm^{-1} for Tl(OH)$_2$, which exhibit +5.0%, +5.4%, +5.7%, and +6.3% differences between calculated harmonic and observed matrix frequencies. Such differences are in line with our previous observations for metal dihydroxides[14,15] and that expected for the B3LYP density functional.[39,40] However, with anharmonic corrections, the differences are reduced to −0.3, 0.7, 1.0, and −2.1%, respectively. The predicted M−O stretching modes at 886.9 cm^{-1} (Al(OH)$_2$), 641.4 cm^{-1} (Ga(OH)$_2$), 564.7 cm^{-1} (In(OH)$_2$), and 397.1 cm^{-1} (Tl(OH)$_2$) are in varying agreement with the observed values (+0.02, −2.4, +2.7, and −11.3%). Furthermore, the symmetric OH bending modes calculated at 634.4 cm^{-1} (Al(OH)$_2$), 820.1 cm^{-1} (Ga(OH)$_2$), 721.5 cm^{-1} (In(OH)$_2$), and 786.7 cm^{-1} (Tl(OH)$_2$ also show a range of agreements with the experimental values (+10.0, +1.3, −5.4, and + 4.8%), and the anharmonic corrections are overkill for this mode. The bending mode intensity is particularly overestimated for the Al and Tl calculations. The M−O−H bending coordinate is clearly more difficult to model mathematically than the simple O−H stretching mode as is shown by the lack of a straightforward relationship between harmonic and anharmonic predictions. In addition, the calculations in Table 3 show that the antisymmetric MOH bending mode is much weaker than the symmetric counterpart and that the former modes are not

observed here. The SDD pseudopotential is, of course, only an approximation as is shown by the underestimation of the Tl−O stretching mode. Higher level theoretical calculations should be performed for these group 13 dihydroxide molecules, as have been done for the metal monohydroxides.[8−10]

Stable $M(OH)_2$ molecules are produced through energized metal atom reactions with H_2O_2 and relaxed and trapped in solid argon (reaction 2), and the exothermic calculated reaction energies are 155, 109, 104, and 66 kcal/mol for Al, Ga, In, and Tl, respectively.

$$M + H_2O_2 \rightarrow [M(OH)_2]^* \text{ matrix relax} \rightarrow M(OH)_2 \quad (2)$$

Calculations were done for the $M(OH)_2^+$ cations to check for this possible product since such cations were prominant in the group 3 spectra.[15a,b] The strong antisymmetric O−H stretching frequencies were computed to be 60−100 cm^{-1} lower for the cations than for the neutral Ga, In, and Tl dihydroxides, just as for group 3, and the cation for Al was predicted to be 2 cm^{-1} above, but here, no such bands are observed. Unfortunately, the ionization energies of the group 13 dihydroxides are about 40 kcal/mol higher than for the group 3 dihydroxides, and our UV lamp cannot drive the matrix photoionization process. The computed structures are interesting as the group 13 dihydroxide cations are isoelectronic with the group 12 dihydroxide molecules[15e] and the C_2 symmetry structures for these species are similar.[41]

$M(OH)_3$. Three new bands at 3752.4 cm^{-1} in the O−H stretching region, at 921.5 cm^{-1} in the Al−O stretching region, and at 655.0 cm^{-1} in the O−H bending region are weak on sample deposition in the reaction of Al with H_2O_2 in solid argon, but these bands are increased 3-fold on annealing to 20 K, decreased on full-arc irradiation, and restored by 30 K annealing (Figure 1). Following the analogous behavior found for the group 3 $M(OH)_3$ reaction product,[15a,b] these bands can be assigned to $Al(OH)_3$. With D_2O_2, the upper two bands shift to 2767.1 and 910.9 cm^{-1}, respectively, and the lower band is too weak to be observed. Obviously, the highest band arises from the O−H stretching mode (H/D ratio 1.3561), and the 921.5 cm^{-1} band is due to the Al−O stretching vibration.

Analogous absorptions for $Ga(OH)_3$ were observed at 3672.4 cm^{-1} (O−H stretching), 850.1 cm^{-1} (O−H bending), and 721.4 and 719.1 cm^{-1} (Ga−O stretching with resolved gallium isotopic components). These bands appeared on deposition and are increased 3-fold on full-arc irradiation. With D_2O_2, the O−H stretching and bending modes shift to 2708.3 and 635.6 cm^{-1}, giving 1.3560 and 1.3375 H/D ratios, respectively, while the Ga−O stretching mode only shifts 0.7 cm^{-1} to 720.7 and 718.3 cm^{-1}. The centrally located Ga−O stretching mode is almost uncoupled to the O−H and O−D bending vibrations. Diagnostic information for the assignment of $Ga(OH)_3$ comes from the mixed H/D peroxide sample. The mixed H_2O_2 and D_2O_2 spectrum reveals two new weak bands at 844.0 and 837.8 cm^{-1} in the O−H bending region and at 651.4 and 643.2 cm^{-1} in the O−D bending region. This isotopic pattern matches that calculated for one or two H substituted by D in the $Ga(OH)_3$ molecule, namely, for $Ga(OH)_2(OD)$ and $Ga(OH)(OD)_2$.

Indium trihydroxide, $In(OH)_3$, is identified through the O−H stretching mode at 3654.7 cm^{-1}, the O−H bending mode at 812.9 cm^{-1}, and the In−O stretching mode at 608.2 cm^{-1} in the laser-ablated In atom reaction with H_2O_2. These bands increased together on irradiation and annealing. The absorptions for $In(OD)_3$ are found at 2695.3 cm^{-1} (O−D stretching), 620.3 cm^{-1} (O−D bending), and 531.4 cm^{-1} (In−O stretching). Note that the H/D ratios for O−H stretching and bending modes are 1.3560 and 1.3105, respectively. The In−O stretching mode shows a 1.1455 ratio, which arises from interaction between the doubly degenerate In−O−D bending and In−O stretching modes of the same symmetry. This interaction does not happen for $In(OD)_2$ since the nearby frequency stretching and bending modes are not of the same symmetry (Table 3). The identification of $In(OH)_3$ is confirmed by the relationship of the observed and calculated O−H stretching and bending modes and In−O stretching modes for $In(OH)_3$ and $In(OH)_2$.

In like fashion, a weak band appears at 3612.2 cm^{-1} just above the 3604.6 cm^{-1} absorption for $Tl(OH)_2$ in hydrogen peroxide experiments, but this band decreases on UV irradiation, unlike the previous $M(OH)_3$ absorptions (Figure 2), and increases on annealing, like the previous $M(OH)_3$ absorptions. The deuterium peroxide counterpart at 2664.6 cm^{-1} defines the appropriate 1.3556 H/D ratio. Associated absorptions in the bending region are found at 790.3 and 590.4 cm^{-1}, which give a 1.3386 H/D ratio. These bands can be assigned to $Tl(OH)_3$ based on their relationship with the absorptions for thallium dihydroxide.

These assignments are supported by DFT frequency calculations (Table 5). The strong antisymmetric O−H stretching modes of $M(OH)_3$ are calculated slightly higher than these modes for $M(OH)_2$ (e.g., 3934.6 cm^{-1} for $Al(OH)_3$, 3861.7 cm^{-1} for $Ga(OH)_3$, 3881.3 cm^{-1} for $In(OH)_3$, and 3849.4 cm^{-1} for $Tl(OH)_3$), which show very similar differences between calculated and observed values as the harmonic $M(OH)_2$ calculations. However, with anharmonic corrections, the calculated frequencies match the experimental measurements more closely. The group 13 trihydroxides have the same C_{3h} structure as the group 3 analogues, although the O−H stretching frequencies are about 100 cm^{-1} lower for the group 13 species and the M−O−H angles are bent to smaller obtuse angles.

The mono- and dihydroxide molecules can react further with H_2O_2 to form trihydroxides. Recall that the trihydroxide molecule absorptions increase on annealing at the expense of the dihydroxide molecules, which requires a spontaneous reaction. This behavior was observed for the group 3 hydroxides.[15a,b] Reaction 3 is exothermic by 152, 98, 93, and 40 kcal/mol for Al, Ga, In, and Tl, respectively. Reaction 4 is exothermic by 78 kcal/mol for Al, 51 kcal/mol for Ga, 45 kcal/mol for In, but only 16 kcal/mol for Tl. The less favorable thermochemistry for Tl no doubt owes to the decreased stability for the III oxidation state on going down the group. Nevertheless, in the presence of a reasonable yield of $Tl(OH)_2$, reaction 4 produced a small increase in $Tl(OH)_3$ on sample annealing. In contrast to group 3, the OMOH molecules were not observed in the present group 13 reaction systems. We note that the dehydration reaction 5 is more endothermic for Al (87 kcal/mol) than for Sc (74 kcal/mol),[15a] and this may account for the greater stability of $Al(OH)_3$ towards decomposition.

$$MOH + H_2O_2 \rightarrow M(OH)_3 \quad (3)$$

$$M(OH)_2 + H_2O_2 \rightarrow M(OH)_3 + OH \quad (4)$$

$$Al(OH)_3 \rightarrow OAlOH + HOH \quad (5)$$

$HAl(OH)_2$. A new group of bands at 3755.0, 1935.7, 911.4, and 511.7 cm^{-1} increase together dramatically on UV irradiation and become the dominant product in Al + H_2 + O_2 experiments, but with Al + H_2O_2, these bands were very weak on sample deposition although they increased on UV irradiation. The deuterium counterparts were found at 2769.4, 1411.5, and 893.5 cm^{-1} with Al + D_2 + O_2. Obviously, the 1935.7 and 1411.5

cm^{-1} bands are appropriate for Al−H and Al−D stretching frequencies (H/D = 1.3714). Recall that similar ratios were found for aluminum hydride molecules (1.3664, i.e., aluminum trihydride)[32,35] but that this Al−H stretching frequency is higher than that even for AlH_3 (1882.6 cm^{-1}), indicating a more positive Al center. The 911.4 cm^{-1} band showing a 17.5 cm^{-1} red-shift in the $D_2 + O_2$ experiment is assigned to the Al−O stretching mode, which is close to the same mode of $Al(OH)_2$. The Al−O−H bending mode absorption at 511.7 cm^{-1} shifts out of our measurement region on deuteriation.

With $H_2 + {}^{18}O_2$, the O−H stretching mode (3755.0 cm^{-1}) shifts to 3743.2 cm^{-1}, the Al−O stretching mode (911.4 cm^{-1}) shifts to 889.9 cm^{-1} (16:18 ratio 1.02416), and the O−H bending mode (511.7 cm^{-1}) shifts to 510.5 cm^{-1}, while no shift was observed for the Al−H stretching mode. The oxygen isotopic triplet pattern with ${}^{16}O_2 + {}^{16}O{}^{18}O + {}^{18}O_2 + H_2$ for the Al−O stretching mode shows that two equivalent oxygen atoms are involved, a conclusion also reached by the Rice group who observed the three lower frequency absorptions and proposed this molecule as the most likely assignment. Therefore, the present observations of the O−H (O−D) and Al−D stretching modes provide further evidence for identification of the $HAl(OH)_2$ molecule.

This assignment is strongly supported by our DFT calculations. With the B3LYP functional, the harmonic O−H stretching mode of $HAl(OH)_2$ with strong intensity is predicted at 3944.6 cm^{-1}, which is 5.0% higher than the observed value. The Al−H stretching mode calculated at 2030.4 cm^{-1} is 4.9% higher than the experimental measurement, which is in very good agreement with previous aluminum hydride calculations.[32] However, the Al−O stretching mode predicted at 901.1 cm^{-1} is underestimated by 10 cm^{-1}. The calculated Al−O−H bending mode also matches the experimental value within the limits expected for the DFT calculation.[39,40]

The $HAl(OH)_2$ product dominates in aluminum atom reactions with $H_2 + O_2$ under UV irradiation, suggesting that the primary reaction is Al and H_2 first giving AlH and then AlH_3, which reacts rapidly with O_2 to form $HAl(OH)_2$. This mechanism receives some support from our lack of observation of the stable calculated $HGa(OH)_2$ molecule in the absence of the necessary GaH_3 reagent, although GaH was formed in these experiments. The indium analogue was not observed as InH was the only hydride produced. In addition, the analogous $HY(OH)_2$ molecule was observed in both $H_2 + O_2$ and H_2O experiments,[13g, 15b] and this only group 3 example of such a structure came along with the highest yield of metal hydride molecules.

$$Al + H_2 \rightarrow AlH + H \quad (6)$$

$$AlH + H_2 \rightarrow AlH_3 \quad (7)$$

$$AlH_3 + O_2 \rightarrow HAl(OH)_2 \quad (8)$$

This mechanism is different from most transition metal atom reactions with $H_2 + O_2$ mixtures, in which metal dioxides, MO_2, are formed first and then react further with H_2 to give the metal dihydroxide molecules, $M(OH)_2$.[14,15] In fact, both AlH_3 and AlO_2 are formed as intermediate precursors ready to react further with O_2 or H_2 (Figure 4), but AlO_2 is more stable, while AlH_3 is more reactive under the conditions of these experiments.

Group Comparisons. First, notice the steady decrease in the O−H stretching frequency from 3788 to 3664 to 3648 to 3605 cm^{-1} in the $M(OH)_2$ series going down the group 13 family from Al to Tl (Figure 2). Similar decreases in frequency going down the row have been observed for the group 2, 3, 11, 12, and 14 metal dihydroxide molecules.[14,15] A similar decrease is observed for the $M(OH)_3$ series as these frequencies are 14, 9, 7, and 6 cm^{-1} above their corresponding dihydroxide values given previously. It is interesting to consider the trend in ionic character in the group series, but the present experimental observation of the O−H stretching frequency is not in itself a measure of ionic character, as discussed previously.[15d] The bent M−O−H bond has been suggested as a sign of covalent character,[42] and in contrast, the more ionic group 2 metal dihydroxides have essentially linear M−O−H bonds.[14a] The quasi-linear AlOH molecule would appear to be more ionic than the bent GaOH molecule,[8,9] and our calculated Mulliken charges on the metals (Al, 0.37 and Ga, 0.26) are in agreement. The M−O−H angles in the dihydroxides (Figure 7) show a small decrease down the family, and the Mulliken charges on the metals are reasonably close, particularly considering that the SDD basis was used for In and Tl (Al, 0.66; Ga, 0.68; In, 0.62; Tl, 0.74).

Second, notice the decrease in the antisymmetric M−O stretching frequency in the $M(OH)_2$ series from 886.7 cm^{-1} for Al to 447.9 cm^{-1} for Tl (Figure 2). The symmetric M−O−H bending mode frequency decreases slightly from 809.2 cm^{-1} for Ga to 750.6 cm^{-1} for Tl but is much lower at 576.7 cm^{-1} for $Al(OH)_2$. The lower frequency and larger M−O−H angle point to more ionic character for $Al(OH)_2$ just as found for AlOH.[8,9]

The C_{2v} structures of group 13 metal dihydroxides determined from a match of observed spectra and calculated spectra for this structure fall between the C_2 structures for the group 12 species and the C_s geometry found for the two heavy group 14 dihydroxides.[14c,15e] The trihydroxides of group 13 share the C_{3h} structure with the group 3 trihydroxides and form from the spontaneous reaction with more H_2O_2 on annealing.

Conclusion

The metal atoms Al, Ga, In, and Tl excited by laser ablation or UV irradiation react with H_2O_2 and with $H_2 + O_2$ mixtures in excess argon to produce new molecules characterized by absorptions in the O−H and M−O stretching and the O−H bending regions, which are assigned to metal mono-, di-, and trihydroxide molecules. Isotopic substitutions (D_2O_2, ${}^{18}O_2$, ${}^{16,18}O_2$, HD, and D_2) and DFT vibrational frequency calculations substantiate these assignments. Spectra for the Al(OH)(OD) molecule verify the calculated C_{2v} structure. Sample annealing allows further reaction to form the trihydroxide molecules that have C_{3h} structures. Excited aluminum atom reactions with $H_2 + O_2$ mixtures favor the $HAl(OH)_2$ product, which suggests that AlH_3 generated by UV irradiation in the cold argon matrix combines readily with O_2 to form $HAl(OH)_2$.

Acknowledgment. We gratefully acknowledge financial support for this research from the National Science Foundation.

References and Notes

(1) (a) Smith, R. W. *Coord. Chem. Rev.* **1996**, *149*, 81. (b) Helm, L.; Merbach, A. E. *Coord. Chem Rev.* **1999**, *187*, 151. (c) Swaddle, T. W.; Rosenqvist, J.; Yu, P.; Bylaska, E.; Phillips, B. L.; Casey, W. H. *Science* **2005**, *308*, 1450.

(2) Richens, D. T. *The Chemistry of Aqua Ions*; Wiley: New York, 1997.

(3) Martin, R. B. *J. Inorg. Biochem.* **1991**, *44*, 141.

(4) (a) Apponi, A. J.; Barclay, W. L.; Ziurys, L. M. *Astrophys. J.* **1993**, *414*, 129. (b) Pilgrim, J. S.; Robbins, D. L.; Duncan, M. A. *Chem. Phys. Lett.* **1993**, *202*, 203.

(5) Lakin, N. M.; Brown, J. M.; Beattie, I. R.; Jones, P. J. *J. Chem. Phys.* **1994**, *100*, 8546.

(6) Hauge, R. H.; Kauffman, J. W.; Margrave, J. L. *J. Am. Chem. Soc.* **1980**, *102*, 6005.

(7) Macrae, V. A.; Downs, A. J. *Phys. Chem. Chem. Phys.* **2004**, *6*, 4571.

(8) (a) Li, S.; Sattelmeyer, K. W.; Yamaguchi, Y.; Schaefer, H. F., III. *J. Chem. Phys.* **2003**, *119*, 12830. (b) Hanady, N. C.; Carter, S.; Yamaguchi, Y.; Turney, J. M.; Schaefer, H. F., III. *Chem. Phys. Lett.* **2006**, *427*, 14.

(9) Richards, C. A.; Yamaguchi, Y.; Kim, S. J.; Schaefer, H. F., III. *J. Chem. Phys.* **1996**, *104*, 8516.

(10) Arulmozhiraja, S.; Fujii, T.; Tokiwa, H. *J. Phys. Chem. A* **1999**, *103*, 4085.

(11) Knight, L. B., Jr.; Woodward, J. R.; Kird, T. J.; Arrington, C. A. *J. Phys. Chem.* **1993**, *97*, 1304.

(12) Cramer, C. J. *J. Mol. Struct.* **1991**, *235*, 243.

(13) (a) Zhang, L.; Dong, J.; Zhou, M. *J. Phys. Chem. A* **2000**, *104*, 8882 (Sc + H_2O). (b) Zhou, M.; Zhang, L.; Dong, J.; Qin, Q. *J. Am. Chem. Soc.* **2000**, *122*, 10680, **2001**, *123*, 135 (Ti, V + H_2O). (c) Zhang, L.; Zhou, M.; Shao, L.; Wang, W.; Fan, K.; Qin, Q. *J. Phys. Chem.* **2001**, *105*, 6998 (Fe + H_2O). (d) Zhou, M.; Zhang, L.; Shao, L. M.; Wang, W.; Fan, K.; Qin, Q. *J. Phys. Chem. A* **2001**, *105*, 5801 (Mn + H_2O). (e) Kauffman, J. W.; Hauge, R. H.; Margrave, J. L. *J. Phys. Chem.* **1985**, *89*, 3541 (Cr−Zn + H_2O). (f) Kauffman, J. W.; Hauge, R. H.; Margrave, J. L. *J. Phys. Chem.* **1985**, *89*, 3547 (Sc, Ti, V + H_2O). (g) Zhang, L.; Shao, L.; Zhou, M. *Chem. Phys.* **2001**, *272*, 27 (Y, La + H_2O).

(14) (a) Andrews, L.; Wang, X. *Inorg. Chem.* **2005**, *44*, 11. (b) Wang, X.; Andrews, L. *J. Phys. Chem. A* **2005**, *109*, 2782 (group 2 metals + H_2O_2). (c) Wang, X.; Andrews, L. *J. Phys. Chem. A* **2005**, *109*, 9013 (Pb, Sn + H_2O_2).

(15) (a) Wang, X.; Andrews, L. *J. Phys. Chem. A* **2006**, *110*, 1850 (Sc + H_2O_2). (b) Wang, X.; Andrews, L. *J. Phys. Chem. A* **2006**, *110*, 4157 (Y, La + H_2O_2). (c) Wang, X.; Andrews, L. *J. Phys. Chem. A* **2005**, *109*, 10689 (group 4 + H_2O_2). (d) Wang, X.; Andrews, L. *Inorg. Chem.* **2005**, *44* (Cu, Ag, Au + H_2O_2). (e) Wang, X.; Andrews, L. *J. Phys. Chem. A* **2005**, *109*, 3849 (Zn, Cd, Hg + H_2O_2).

(16) Andrews, L. *Chem. Soc. Rev.* **2004**, *33*, 123.

(17) Andrews, L.; Citra, A. *Chem. Rev.* **2002**, *102*, 885.

(18) Pettersson, M.; Tuominen, S.; Rasanen, M. *J. Phys. Chem. A* **1997**, *101*, 1166.

(19) Pehkonen, S.; Pettersson, M.; Lundell, J.; Khriachtchev, L.; Rasanen, M. *J. Phys. Chem. A* **1998**, *102*, 7643.

(20) Kudin, K. N.; Burant, J. C.; Millam, J. M.; Iyengar, S. S.; Tomasi, J.; Barone, V.; Mennucci, B.; Cossi, M.; Scalmani, G.; Rega, N.; Petersson, G. A.; Nakatsuji, H.; Hada, M.; Ehara, M.; Toyota, K.; Fukuda, R.; Hasegawa, J.; Ishida, M.; Nakajima, T.; Honda, Y.; Kitao, O.; Nakai, H.; Klene, M.; Li, X.; Knox, J. E.; Hratchian, H. P.; Cross, J. B.; Adamo, C.; Jaramillo, J.; Gomperts, R.; Stratmann, R. E.; Yazyev, O.; Austin, A. J.; Cammi, R.; Pomelli, C.; Ochterski, J. W.; Ayala, P. Y.; Morokuma, K.; Voth, G. A.; Salvador, P.; Dannenberg, J. J.; Zakrzewski, V. G.; Dapprich, S.; Daniels, A. D.; Strain, M. C.; Farkas, O.; Malick, D. K.; Rabuck, A. D.; Raghavachari, K.; Foresman, J. B.; Ortiz, J. V.; Cui, Q.; Baboul, A. G.; Clifford, S.; Cioslowski, J.; Stefanov, B. B.; Liu, G.; Liashenko, A.; Piskorz, P.; Komaromi, I.; Martin, R. L.; Fox, D. J.; Keith, T.; Al-Laham, M. A.; Peng, C. Y.; Nanayakkara, A.; Challacombe, M.; Gill, P. M. W.; Johnson, B.; Chen, W.; Wong, M. W.; Gonzalez, C.; Pople, J. A. *Gaussian 03*, revision B.04; Gaussian, Inc.: Pittsburgh, PA, 2003 and references therein.

(21) (a) Becke, A. D. *J. Chem. Phys.* **1993**, *98*, 5648. (b) Lee, C.; Yang, W.; Parr, R. G. *Phys. Rev. B* **1988**, *37*, 785.

(22) Frisch, M. J.; Pople, J. A.; Binkley, J. S. *J. Chem. Phys.* **1984**, *80*, 3265.

(23) Andrae, D.; Haeussermann, U.; Dolg, M.; Stoll, H.; Preuss, H. *Theor. Chim. Acta* **1990**, *77*, 123.

(24) Page, M.; Doubleday, C.; McIver, J. W., Jr. *J. Chem. Phys.* **1990**, *93*, 5634.

(25) (a) Reddington, R. L.; Milligan, D. E. *J. Chem. Phys.* **1962**, *37*, 2162. (b) Ayers, G. P.; Pullen, A. D. E. *Spectrohim. Acta* **1976**, *32*, 1629.

(26) Zhou, M.; Hacalogu, J.; Andrews, L. *J. Chem. Phys.* **1999**, *110*, 9450.

(27) Milligan, D. E.; Jacox, M. E. *J. Mol. Spectrosc.* **1973**, *46*, 460.

(28) Jacox, M. E.; Thompson, W. E. *J. Chem. Phys.* **1994**, *100*, 750.

(29) Chertihin, G. V.; Bare, W. D.; Andrews, L. *J. Chem. Phys.* **1997**, *107*, 2798.

(30) (a) Bare, W. D.; Souter, P. F.; Andrews, L. *J. Phys. Chem. A* **1998**, *102*, 8279. (b) Zhou, M.; Andrews, L. *J. Chem. Phys.* **1999**, *111*, 4230.

(31) Andrews, L.; Burkholder, T. R.; Yustein, J. T. *J. Phys. Chem.* **1992**, *96*, 10182.

(32) (a) Chertihin, G. V.; Andrews, L. *J. Phys. Chem.* **1993**, *97*, 10295. (b) Andrews, L. Wang, X. *J. Phys. Chem. A* **2004**, *108*, 4202.

(33) Burkholder, T. R.; Yustein, J. T.; Andrews, L. *J. Phys. Chem.* **1992**, *96*, 10189.

(34) Wang, X.; Andrews, L. *J. Phys. Chem.* **2003**, *107*, 11371.

(35) (a) Pullumbi, P.; Mijoule, C.; Manceron, L.; Bouteiller, Y. *Chem. Phys.* **1994**, *185*, 13. (b) Pullumbi, P.; Bouteiller, Y.; Manceron, L.; Mijoule, C. *Chem. Phys.* **1994**, *185*, 25.

(36) Andrews, L.; Kushto, G. P.; Yustein, J. T.; Archibong, E.; Suillivan, R.; Leszczynski, J. *J. Phys. Chem.* **1997**, *101*, 9077.

(37) (a) Burkholder, T. R.; Andrews, L. *J. Chem. Phys. Chem.* **1991**, *95*, 8697. (b) Andrews, L.; Burkholder, T. R. *J. Phys. Chem.* **1991**, *95*, 8554. (c) Tague, T. J., Jr.; Andrews, L. *J. Am. Chem. Soc.* **1994**, *116*, 4970.

(38) Andrews, L.; Burkholder, T. R. *J. Chem. Phys.* **1992**, *97*, 7203.

(39) Scott, A. P.; Radom, L. *J. Phys. Chem.* **1996**, *100*, 16502.

(40) Andersson, M. P.; Uvdal, P. L. *J. Phys. Chem. A* **2005**, *109*, 2937.

(41) Parameters calculated for the $M(OH)_2^+$ cation C_2 structures for the O−H and M−O bond lengths and the M−O−H and O−M−O dihedral angles, in angstroms and degrees, respectively: Al, 0.957, 1.605, 153, 174, 171; Ga, 0.969, 1.708, 120, 145, 84; In, 0.966, 1.873, 121, 145, 84; and Tl, 0.968, 1.919, 116, 142, 65.

(42) (a) Ikeda, S.; Nakajima, T.; Hirao, K. *Mol. Phys.* **2003**, *101*, 105 and references therein. (b) Bauschlicher, C. W., Jr. *Int. J. Quantum Chem. Symp.* **1986**, *20*, 563.